

Non-thermal emission from massive YSOs. Exploring the spectrum at high energies

Anabella T. Araudo^{1,2}, Gustavo E. Romero^{1,2}, Valentí Bosch-Ramon³
and Josep M. Paredes⁴

*1 Instituto Argentino de Radioastronomía, (CCT La Plata - CONICET)
Casilla de Correos No. 5, Villa Elisa 1894, Provincia de Buenos Aires
ARGENTINA. E-mail: aaraudo@fcaglp.unlp.edu.ar*

*2 Facultad de Cs. Astronómicas y Geofísicas, Universidad Nacional de
La Plata, Paseo del Bosque, 1900 La Plata, Argentina*

*3 Max Planck Institut für Kernphysik, Saupfercheckweg 1, Heidelberg
69117, Germany*

*4 Departament d'Astronomia i Meteorologia, Universitat de Barcelona,
Martí i Franquès 1, 08028, Barcelona, Spain*

Abstract. Thermal radio and X-ray emission has been traditionally associated with the formation of stars. However, in recent years, non-thermal radiation from massive star forming regions has been detected.

Synchrotron radio emission and non-thermal X-rays from the outflows of massive young stellar objects (YSOs) provide evidence of the presence of relativistic particles in these sources. In YSOs, the acceleration of particles is likely produced where the thermal jet impacts on the surrounding medium and a shock wave is formed. Thus, particles might be accelerated up to relativistic energies through a Fermi-I type mechanism.

Relativistic electrons and protons can interact with thermal particles and photons, producing then γ -rays. These energetic photons could be detected by the new generation of instruments, making massive YSOs a new population of γ -ray sources.

In the present contribution we briefly describe some massive star forming regions from which non-thermal radio emission has been detected. In addition, we present a general model for high-energy radiation from the massive YSOs embedded in these regions. We take into account both leptonic and hadronic interactions of particles accelerated at the termination points of the collimated outflows ejected from the protostar.

1. Introduction

The mechanism of formation of massive stars ($M > 8M_{\odot}$) remains one of the open questions in astrophysics. Massive stars appear in massive star associations where cloud fragmentation seems to be common. It is known that these stars originate inside giant and massive molecular clouds but the sequence of processes that take place during the formation of the star are mostly unknown. It has

been suggested, for example, that the coalescence of various protostars in the same cloud can lead to the emergence of a massive star (Bonnell et al. 1998). Alternatively, a massive star could form by the collapse of the core of a molecular cloud, with associated episodes of mass accretion and ejection, as observed in low-mass stars (Shu et al. 1987). In such a case, the effects of jets propagating through the medium that surrounds the protostar should be detectable.

Until now, the formation of stars has been mostly associated with thermal radio and X-ray emission. However, non-thermal radio emission has been detected in some massive star forming regions. This is a clear evidence that efficient particle acceleration is occurring there, which may have as well a radiative outcome at energies much higher than radio ones.

In the present contribution, based on recent multiwavelength observations and reasonable physical assumptions, we show that massive protostars could produce a significant amount of radiation in the gamma-ray domain, because of the dense and rich medium in which they are formed.

2. Non-thermal radio sources

In recent years, synchrotron radiation has been observed from some regions where massive stars form. This emission is associated with outflows emanating from a central protostar. In what follows, we briefly describe some of these non-thermal radio sources that could be potential emitters of gamma-rays.

2.1. IRAS 16547–4247

The triple radio source associated with the protostar IRAS 16547–4247 is one of the best candidates to produce gamma-rays. This system is located within a very dense region (i.e. densities $n \approx 5 \times 10^5 \text{ cm}^{-3}$) of a giant molecular cloud located at a distance of 2.9 kpc. The luminosity of the IRAS source is $L = 6.2 \times 10^4 L_\odot$, possibly being the most luminous known YSO associated with collimated thermal jets.

ATCA and VLA observations (Garay et al. 2003, Rodríguez et al. 2005) have shown that the southern lobe of this system, of size $\sim 10^{16} \text{ cm}$, has a clear non-thermal spectrum, with an index $\alpha \sim 0.6$ ($S_\nu \propto \nu^{-\alpha}$). The specific flux of this source is 2 mJy at 14.9 GHz and the estimated magnetic field is $B \sim 2 \times 10^{-3} \text{ G}$ (Araudo et al. 2007).

2.2. Serpens

The Serpens molecular cloud is located at a distance of $\sim 300 \text{ pc}$. One of the two central dense cores of this cloud is a triple radio source, composed by a central protostar (IRAS 18273–0113) and two lobes. The northwest (NW) hot-spot is connected with the central source by a highly collimated thermal jet, whereas the southeast (SE) is separated and broken into two clumps. The luminosity of the source IRAS 18273–0113 is $L \sim 300 L_\odot$ and the particle density at the center of the molecular cloud is $n_0 \sim 10^5 \text{ cm}^{-3}$.

The observed radio emission (Rodríguez et al. 1989, Curiel et al. 1993) detected from the central and NW sources has a spectral index $\alpha \approx -0.15$ and $\alpha \approx 0.05$, respectively. This emission, of a luminosity $\sim 2 - 3 \text{ mJy}$, is produced

via thermal Bremsstrahlung. However, the radiation produced in the SE lobe seems to be non-thermal ($\alpha = 0.3$), likely produced via synchrotron emission. The specific flux of this source is $2 - 5$ mJy. The equipartition magnetic field estimated in the SE lobe is $B_{\text{equip}} \sim 10^{-3}$ G (Rodríguez et al. 1989).

2.3. HH 80-81

The famous Herbig-Haro objects called HH 80–81 are the south component of a system of radio sources located in the Sagittarius region, at a distance of 1.7 kpc. The central source has been identified with the luminous ($L = 1.7 \times 10^4 L_{\odot}$) protostar IRAS 18162–2048. HH 80 North is the northern counterpart of HH 80–81. The velocity of the jet has been estimated as $v \sim 700$ km s $^{-1}$, allowing to derive a dynamical age for the system similar to 4000 yr.

Radio observations carried out with the VLA instrument (Martí et al. 1993) showed that the central source has a spectral index $\alpha \sim 0.1$, typical of free-free emission, whereas HH 80–81 and HH 80 North are likely non-thermal sources, with spectral index $\alpha \sim 0.3$. The specific flux measured at a frequency of 5 GHz is $F_{\nu} \sim 1 - 2$ mJy and $F_{\nu} \approx 2.4$ mJy for the sources HH 80–81 and HH 80 North, respectively. At this frequency, the angular size of the north and the south components are $\sim 6''$.

In addition, the HH 80–81 system is a source of thermal X-rays with a luminosity $L_X \sim 4.3 \times 10^{31}$ erg s $^{-1}$ (Pravdo et al. 2004).

2.4. W3(OH)

Another interesting source to study is the system composed by an H $_2$ O maser complex and the Turner-Welch (TW) source in the W3 region (Wilner et al. 1999). The central source of this system is a very luminous ($L \sim 10^5 L_{\odot}$) YSO and the mean density of cool particles is $n \sim 4 \times 10^4$ cm $^{-3}$. The distance to W3(OH) is 2.2 kpc.

Continuum radio observations (Wilner et al. 1999) show the presence of a sinuous double-sided jet, emanating from the TW source. The observed radio flux, from 1.6 to 15 GHz, is in the range 2.5–0.75 mJy, and the spectral index of the observed emission is clearly non-thermal: $\alpha = 0.6$. The inhomogeneous synchrotron model proposed by Reid et al. (1995) predicts for the emitting jet a density of relativistic electrons $n_e(\gamma, r) = 0.068\gamma^{-2}(r/r_0)^{-1.6}$ cm $^{-3}$ and a magnetic field $B(r) = 0.01(r/r_0)^{-0.8}$ G, where $r_0 = 6.6 \times 10^{15}$ cm, and r and γ are the distance to the jet origin and the electron Lorentz factor, respectively. Unlike in the previous cases, here the non-thermal radio emission comes from the jet and not from its termination region. Non-thermal jets associated with a YSO are uncommon.

3. Acceleration of particles and losses

The non-thermal radio emission observed in some massive star forming regions is interpreted as synchrotron radiation produced by the interaction of relativistic electrons with the magnetic field present in the cloud, being typically $B_{\text{cloud}} \sim 10^{-3}$ G (Crutcher 1999). These particles could be accelerated at a shock, formed in the point where the jet terminates, via diffusive shock acceleration (Drury

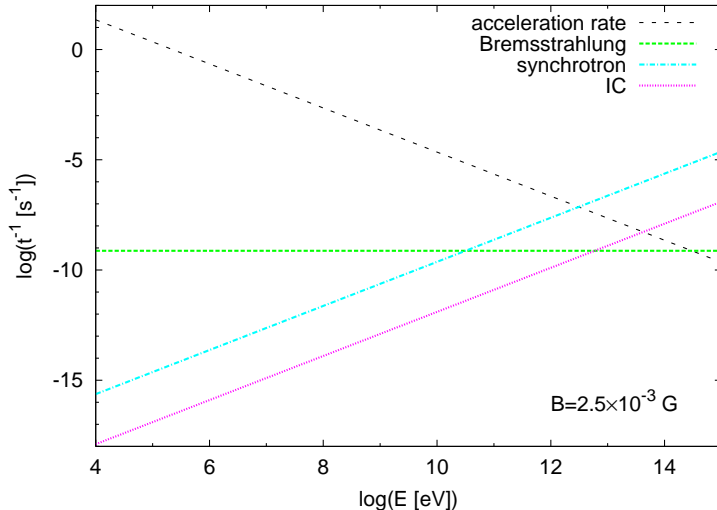


Figure 1. Energy loss and acceleration rates for electrons in the IRAS 16547–4247 southern lobe.

1983). The acceleration efficiency, characterized by η , is related to the velocity of the shock. Using the values of the velocities given for the sources described in the previous section, and assuming Bohm diffusion, values for η of $\sim 10^{-6} - 10^{-5}$ are obtained.

Particles accelerated up to relativistic energies interact with the different fields present in the medium. As noted at the beginning of this section, electrons radiate synchrotron emission under the ambient magnetic field B . In addition, particles, electrons and protons, can also interact with the cold matter in the jet termination region (via relativistic Bremsstrahlung the leptons, and inelastic proton-nuclei collisions the protons). In addition, electrons interact with the background field of IR photons of the protostar, of energy density u_{ph} , through inverse Compton (IC) scattering.

Using the following parameter values: $n = 5 \times 10^5 \text{ cm}^{-3}$; $B = 2.5 - 3 \times 10^{-3} \text{ G}$; and $u_{\text{ph}} = 3.2 \times 10^{-9} \text{ erg cm}^{-3}$ given for IRAS 16547–4247 (Garay et al. 2003, Araudo et al. 2007), we estimate the cooling time of the main leptonic processes in this scenario. As seen in Figure 1, relativistic Bremsstrahlung losses are dominant up to $\sim 10 \text{ GeV}$. In addition, it is possible to see from this figure that the maximum energy achieved by electrons is $E_e^{\text{max}} \sim 4 \text{ TeV}$ and is determined by synchrotron losses, being IC losses negligible.

Protons can be accelerated by the shock in the same way as electrons and interact with cold particles present in the cloud. The maximum energy achieved by protons is higher, $E_p^{\text{max}} \sim 10^2 \text{ TeV}$, and determined by the size of the acceleration region. In pp interactions, besides γ -rays, secondary electron-positron pairs are produced. The maximum energies of these leptons is $E_{e^\pm}^{\text{max}} \sim 10 \text{ TeV}$. These secondary particles will radiate by the same mechanisms as primary electrons (i.e. synchrotron radiation, IC scattering and relativistic Bremsstrahlung).

4. High-energy emission

In order to calculate the non-thermal spectral energy distribution (SED) of a massive protostar, the magnetic field of the cloud and the distributions of relativistic particles, $n(E)$, are needed. To obtain the magnetic field B and the normalization constants of the particle distributions, we use the standard equations given by Ginzburg & Syrovatskii (1964) for the observed synchrotron flux and assume equipartition between the magnetic and the relativistic particle energy densities:

$$\frac{B^2}{8\pi} = u_e + u_p + u_{e\pm}, \quad (1)$$

where u_e , u_p and $u_{e\pm}$ are the energy density of relativistic electrons, protons and secondary pairs, respectively. In Eq. (1), the following relationships are implicit: $u_p = a u_e$ and $u_{e\pm} = f u_p$. The constant a is a free parameter of the model, that characterizes how much energy goes to the different types of accelerated particles and f can be estimated using the average ratio of the number of secondary pairs to π^0 -decay photons as in Kelner et al. (2006).

In Figs. 2 and 3, we show the computed broadband SEDs for the parameters of the source IRAS 16547–4247, in the cases with $a = 1$ (equipartition between protons and electrons) and $a = 100$ (larger acceleration efficiency in protons than in electrons). As seen from these figures, in the former case the leptonic emission is dominated by the primary electron population and in the latter by the secondary pairs. The typical lepton luminosities are $L_e \sim 10^{32}$ erg s⁻¹. Regarding the hadronic emission, the luminosity produced by π^0 -decay is higher in the case $a = 100$, reaching a value of $L_{pp} \sim 5 \times 10^{32}$ erg s⁻¹.

5. Discussion

In this work we show that, if the source is located at few kpc, the high-energy emission may be detected by GLAST and even by forthcoming Cherenkov telescope arrays after long enough exposure. This opens a new window to the study of star formation and related processes. Also, determinations of the particle spectrum and its high-energy for different sources with a variety of environmental conditions can shed light on the properties of galactic supersonic outflows, and on the particle acceleration processes occurring at their termination points.

Radio observations already demonstrate that relativistic electrons are produced in some sources. According to the presence of non-thermal emission detected at cm-wavelengths and IR observations of the protostar emission we can suggest several good candidates to be targeted by GLAST. These objects are IRAS 16547–4247 (Araudo et al. 2007), the multiple radio source in Serpens (Rodríguez et al. 1989, Curiel et al. 1993), HH 80–81 (Martí et al 1993) and W3 (Reid et al. 1995, Wilner et al. 1999).

To conclude, we emphasize that massive YSO with bipolar outflows and non-thermal radio emission can form a new population of gamma-ray sources that could be unveiled by the next generation of γ -ray instruments.

Acknowledgments. A.T.A. and G.E.R. are supported by CONICET (PIP 5375) and the Argentine agency ANPCyT through Grant PICT 03-13291 BID

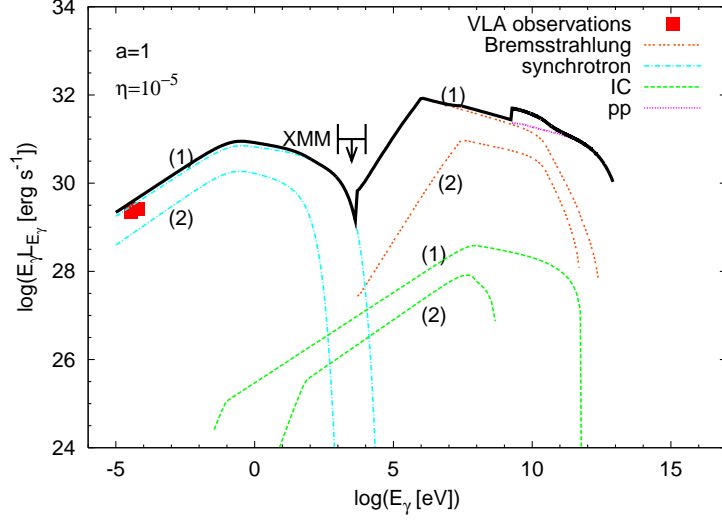


Figure 2. Spectral energy distribution for the south lobe of the YSO embedded in the source IRAS 16547–4247, for the case $a = 1$. The radiative contribution of secondary pairs (2) produced via π^\pm -decay is shown along with the contribution of primary electrons (1).

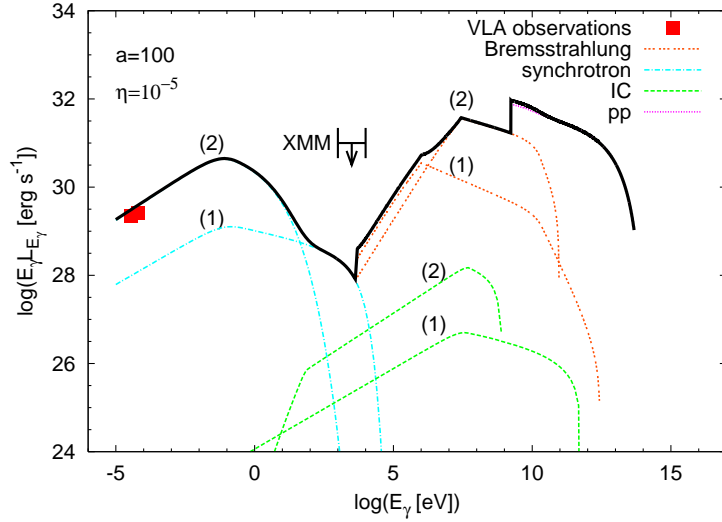


Figure 3. The same as in Fig. 2, but for the case $a = 100$.

1728/OC-AC. V.B-R. gratefully acknowledges support from the Alexander von Humboldt Foundation. V.B-R., and J.M.P acknowledge support by DGI of MEC under grant AYA2004-07171-C02-01, as well as partial support by the European Regional Development Fund (ERDF/FEDER).

References

- A. T. Araudo, G. E. Romero, V. Bosch-Ramon & J. M. Paredes, 2007, *A&A*, 476, 1289
- I. A. Bonnell, M. R. Bate & H. Zinnecker, 1998, *MNRAS* 298, 93
- R. M. Crutcher, 1999, *ApJ*, 520, 706
- S. Curriel, L. F. Rodríguez, J. M. Morán & J. Cantó, 1993, *ApJ*, 415, 191
- L. O’C. Drury, 1983, *Rep. Prog. Phys.*, 46, 973
- G. Garay, K. Brooks, D. Mardones & R. P. Norris, 2003, *ApJ*, 537, 739
- V. L. Ginzburg & S. I. Syrovatskii *The Origin of Cosmic Rays*, Pergamon Press, New York, 1964
- S. R. Kelner, F. A. Aharonian, & V. V. Vugayov, 2006, *Phys. Rev. D*, 74, 034018
- J. Martí, L. F. Rodríguez, & B. Reipurth, 1993, *ApJ*, 449, 184
- S. H. Pravdo, Y. Tsuboi & Y. Maeda, 2004, *ApJ*, 605, 259
- M. J. Reid, A. L. Argon, K. M. Menten, & J. M. Moran, 1995, *ApJ*, 443, 238
- L. F. Rodríguez, S. Curriel, J. M. Morán, I. F. Mirabel, M. Roth & G. Garay, 1989, *ApJ*, 346, L85
- L. F. Rodríguez, G. Garay, K. J. Brooks & D. Mardones, 2005, *ApJ*, 626, 953
- F. H. Shu, F. C. Adams & S. Lizano, 1987, *ARA&A*, 25, 23
- D. J. Wilner, M. J. Reid, & K. M. Menten, 1999, *ApJ*, 513, 775